[3]Krupp, J.A., "The Numerical Calculation of Plane Steady Transonic Flows Past Thin Lifting Airfoils," Boeing Scientific Research Lab. Rept. D180-12958-1, June 1971.

[4]Sirovich, L. and Huo, C., "Simple Waves and the Transonic Similarity Parameter," *AIAA Journal*, Vol. 14, Aug. 1976, pp. 1125-1127.

[5]Germain, P., "Ecoulements Transsoniques Homogenes," *Progress in Aeronautical Sciences*, Vol. 5, Pergamon Press, New York, 1964, pp. 143-273.

[6]Nonweiler, T.R.F., "The Sonic Flow About Some Symmetric Half-Bodies," *Journal of Fluid Mechanics*, Vol. 4, 1958, pp. 140-148.

[7]Murman, E.M. and Cole, J.D., "Calculation of Plane Steady Transonic Flows," *AIAA Journal*, Vol. 9, Jan. 1971, pp. 114-121.

[8]Klunker, E.B. and Newman, P.A., "Computation of Transonic Flow About Lifting Wing-Cylinder Combinations," *Journal of Aircraft*, Vol. 11, April 1974, pp. 254-256.

[9]Jameson, A., "Iterative Solutions of Transonic Flows Over Airfoils and Wings, Including Flows at Mach 1," *CPAM*, Vol. XXVII, 1974, pp. 283-309.

Use of Primitive Variables in the Solution of Incompressible Navier-Stokes Equations

K. N. Ghia*
University of Cincinnati, Cincinnati, Ohio
and
W. L. Hankey Jr.† and J. K. Hodge‡
Air Force Flight Dynamics Laboratory, Wright Patterson AFB, Ohio

I. Introduction

TWO-DIMENSIONAL laminar incompressible flows have been studied extensively by several investigators using the Navier-Stokes equations formulated in terms of vorticity ω and stream function ψ. This formulation, although remarkably useful for two-dimensional flows in simply connected regions, is not easily extendable to three-dimensional, compressible or turbulent flow applications. Two of the alternate formulations which are not as severely handicapped for complex problems are: the velocity-vorticity formulation, and the velocity-pressure formulation.

In the present study, it is planned to develop a method using the primitive variables (u,v,p) to solve the Navier-Stokes equations, with a view to later extending the method to more involved flow configurations. To carry out this task successfully, followed by a complete comparative study of this solution with the (ω,ψ) solution, it is important to choose a meaningful model flow problem. In his recent article, Roache[1] has underscored this point. An essential feature desired in the present model problem is that it be a true Navier-Stokes problem. Therefore, the driven flow in a square cavity is selected as a model problem (see Fig. 1, Ref. 2).

Presented as Paper 77-648 at the AIAA 3rd Computational Fluid Dynamics Conference, Albuquerque, N. Mex., June 27-28, 1977; submitted Oct. 13, 1977; revision received Oct. 6, 1978.

Index categories: Computational Methods; Viscous Nonboundary-Layer Flows.

*Professor of Aerospace Engineering and Applied Mechanics. Member AIAA.

†Senior Scientist, Computational Fluid Dynamics Group. Associate Fellow AIAA.

‡Aerospace Engineer, Computational Fluid Dynamics Group. Member AIAA.

Burggraf[3] studied the cavity-flow problem with great care and provided results for Reynolds number, Re, ranging from zero to 400. Several investigators[4-8] have used the cavity problem as a model problem to test new numerical schemes, as qualitative experimental data[9,10] as well as detailed numerical results[3-5] are available for this problem. The latter is obtained by numerical schemes accurate to second order or higher.[5]

It is recognized that the corner-singularities present in the cavity-flow configuration cause some numerical difficulties. However, it is believed that the effect of these singularities is only local, and the global solution is not affected significantly. Ideally, it would be desirable to treat these singularities analytically and determine the numerical solution such that it matches smoothly with the local analytical solutions at these singular points.[11]

II. Formulation of the Problem

Governing Equations

In convective form, the differential equations governing the cavity-flow problem are:

$$u_x + v_y = 0 \tag{1}$$

$$u_t + uu_x + vu_y = -p_x + (1/Re)(u_{xx} + u_{yy}) \tag{2}$$

$$v_t + uv_x + vv_y = -p_y + (1/Re)(v_{xx} + v_{yy}) \tag{3}$$

Here, the Reynolds number Re is defined as $Re = \rho UL/\mu$, with U being the velocity of the moving wall. All velocities have been made dimensionless with respect to U, pressure with reference to ρU^2, and distances with respect to the width L of the square cavity.

Unfortunately, the pressure p, which is nested in this system, does not appear as a dominant variable in any of these equations. To correctly model the elliptic nature of the flow problem, the pressure p in the (u,v,p) system may be determined from a Poisson equation obtained by appropriately forming the divergence of the vector momentum equation. Thus, the following Poisson equation must replace the continuity equation.

Poisson Equation for Pressure

$$p_{xx} + p_{yy} = S_p - \frac{\partial}{\partial t}[u_x + v_y] \tag{4}$$

where

$$S_p \triangleq \frac{\mathrm{d}}{\mathrm{d}x}\left[-(uu_x + vu_y) + \frac{1}{Re}(u_{xx} + u_{yy})\right] + \frac{\mathrm{d}}{\mathrm{d}y}\left[-(uv_x - vv_y) + \frac{1}{Re}(v_{xx} + v_{yy})\right] \tag{5}$$

The derivatives of the local dilation term $D \triangleq u_x + v_y$ appearing in Eqs. (4) and (5) intentionally have not been set to zero; the reason for doing this will be explained in the next section.

Boundary Conditions

The boundary conditions for the cavity-flow problem in the (u,v,p) system are relatively straightforward (see Fig. 1, Ref. 2). For the momentum equations, the normal velocities are zero at the nonporous walls, while the tangential velocities satisfy the condition of zero slip at all walls. For the pressure equation, the boundary conditions consist of the normal gradient $\partial p/\partial n$ evaluated from the appropriate momentum equation.

III. Results and Conclusion

On the Computational Aspects of the Solution

It should be emphasized that the derivative boundary conditions for pressure, together with Eqs. (4) and (5), lead to a Neumann problem whose solution requires very careful consideration. The solution of this problem has frustrated many analysts[5] and has, therefore, comprised the crux of the present analysis. In the present work, the pressure is obtained by solving the Poisson equation with the Neumann boundary value $\partial p/\partial n$ evaluated at the interior boundary. The existence of a converged solution requires the satisfaction of an integral constraint. This, as well as the detailed treatment of the pressure boundary condition, has been described in Ref. 2.

A two-step, alternating-direction implicit (ADI) method is used for the solution of the momentum equations, with a successive-over-relaxation (SOR) method for the solution of the pressure equation. Second-order accurate central differences are used for all spatial derivatives. The following definition is used for convergence. Using a general variable F to denote the dependent variables u, v, and p, the convergence criterion is expressed as:

$$ABS[1-(F^{*}_{i,j}/F^{n+1}_{i,j})]<\epsilon \tag{6}$$

The value of ϵ selected for the momentum equations is $\epsilon_{u,v}=10^{-5}$, wheres for the Poisson equation for pressure, $\epsilon_p=10^{-10}$.

It was found that an essential requirement for the convergence of the numerical procedure is the retention of the temporal derivative of the local dilation in the Poisson equation for pressure, Eq. (4). Any attempt to totally set this term to zero leads to nonlinear instability in the numerical solution. The work of the researchers at the Los Alamos Laboratory suggests to retain the term $\partial D/\partial t$ in the Poisson equation for pressure. The pressure at the new time step is then determined so as to satisfy $D^{n+1}=0$.

For the check case with $Re=100$, the horizontal velocity u is shown in Fig. 1a. The results were first obtained using a coarse mesh of 15×15; the mesh was then successively refined to 29×29 and, finally, to 57×57 points. The results obtained by Burggraf[3] using a 41×41 grid, with the SOR method for the (ω,ψ) formulation, are also plotted in this figure. In addition to showing the effect of grid size, Fig. 1a indicates that the results of the 29×29 grid agree satisfactorily with those of Burggraf. Therefore, the 29×29 grid may be considered to be the optimum grid for the (u,v,p) system, for $Re=100$. However, as the Reynolds number increases to 400 and beyond, the viscous region near the walls becomes very thin, thus necessitating a fine grid near the walls, for the numerical solution to be reliable. A nonuniform grid in the physical plane is achieved conveniently with the help of analytical transformations such that

$$\xi=a\tan\left(\frac{x-b}{c}\right)+b \tag{7a}$$

$$\eta=a\tan\left(\frac{y-b}{c}\right)+b \tag{7b}$$

where a,b and c are constants evaluated from the geometric conditions for the transformation. This transformation is particularly suitable for the internal-flow configuration of the cavity where boundary layers are encountered at both end boundaries of the coordinates.

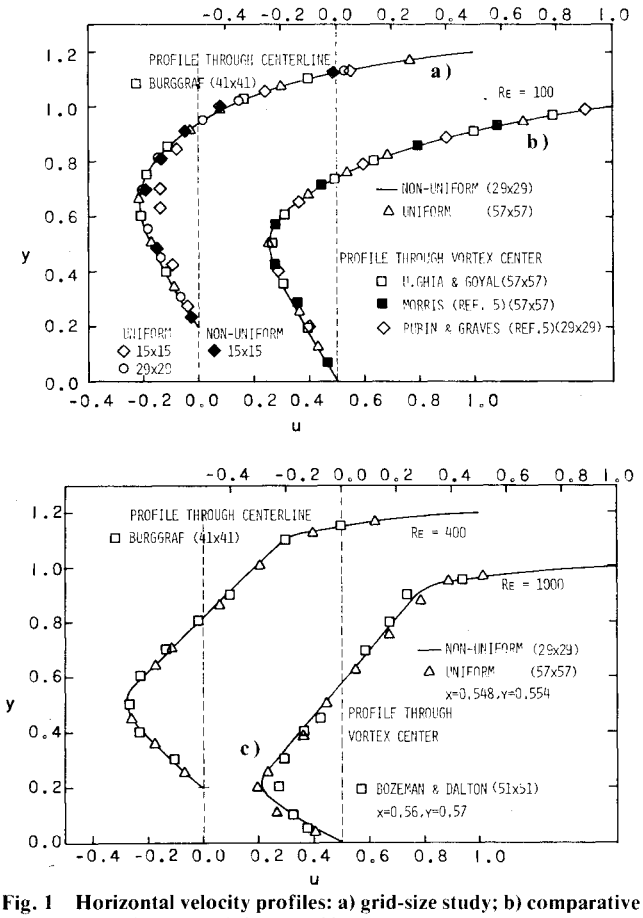

Fig. 1 Horizontal velocity profiles: a) grid-size study; b) comparative study, $Re=100$, c) $Re=400$ and 1000.

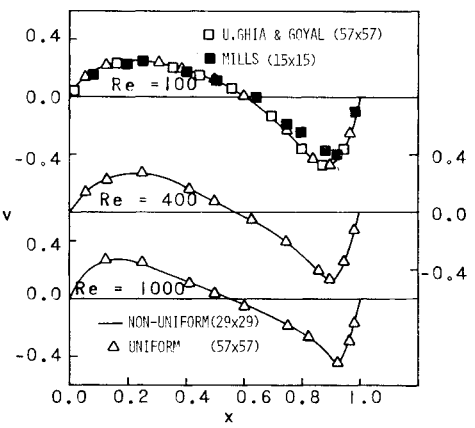

Fig. 2 Vertical velocity profiles through vortex center.

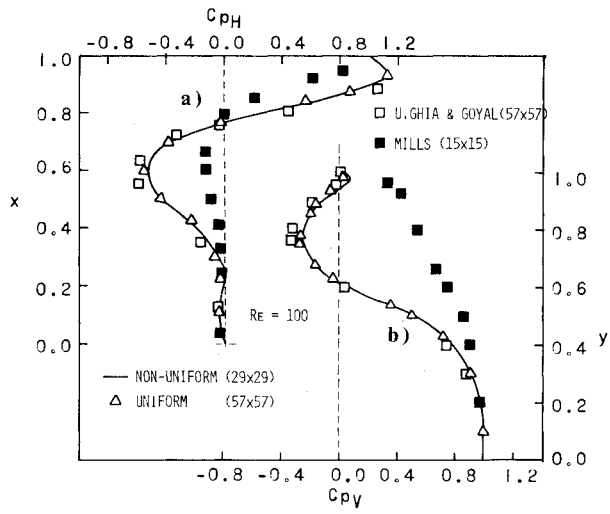

Fig. 3 Pressure coefficient through vortex center: a) horizontal profile; b) vertical profile.

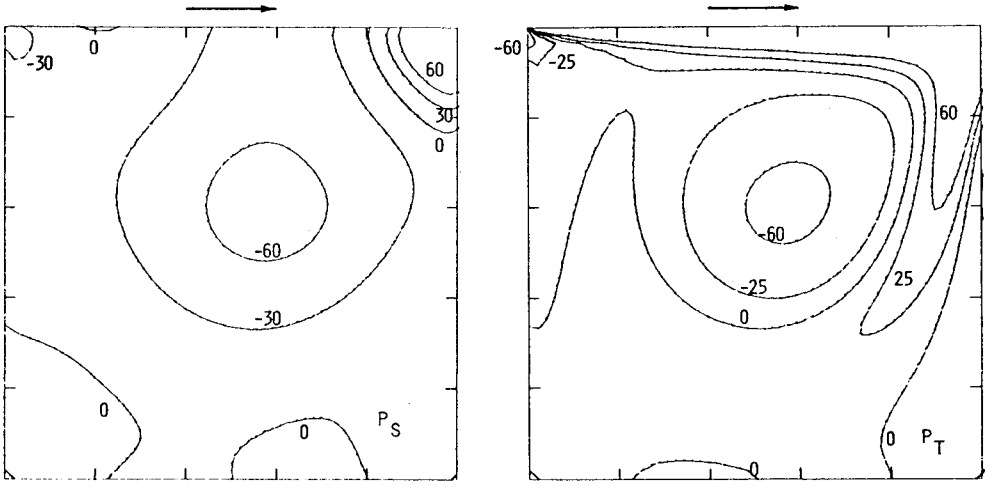

Fig. 4 Contours of static pressure P_S and total pressure P_T, $Re = 400$.

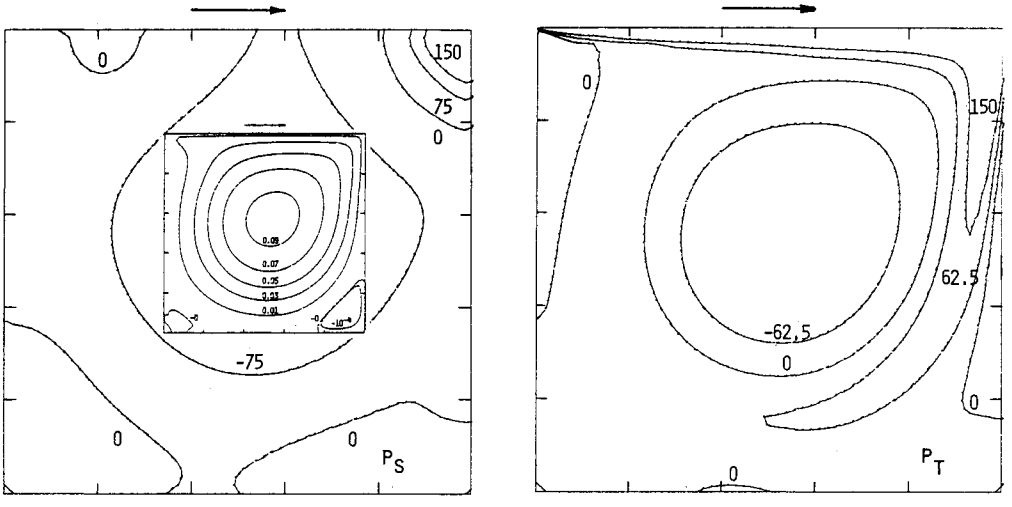

Fig. 5 Contours of static pressure P_S and total pressure P_T, $Re = 1000$ (inset: corresponding streamlines).

Comparative Study

For the case of $Re = 100$, the results for the u-velocity profile at the vertical centerline of the cavity, using a uniform grid of 57×57 and a nonuniform grid of 29×29, are compared in Fig. 1b with three available sets of results; the present results are seen to agree favorably with all of these results. For $Re = 400$ and 1000, comparison of the existing results with the present numerical solutions show close agreement (Fig. 1c). The v-velocity profiles through the vortex center are presented in Fig. 2 for $Re = 100$, 400 and 1000. The agreement between the results for the case of $Re = 100$ and those of Ghia and Goyal[12] is good. However, the results show some discrepancy when compared with those of Mills,[9] the latter results having been generated using only a 15×15 grid. Further, the results for pressure in terms of the pressure coefficients C_{pV} and C_{pH} (see Ref. 2 for definitions), are also compared with the corresponding results of Mills,[9] who integrated the momentum equations expressed in terms of total pressure. The discrepancies observed in Figs. 3b and 3c are quite significant; hence, these results were further scrutinized (see Ref. 2). This examination led the authors to infer that the results of Mills[9] for C_{pV} and C_{pH} shown in Fig. 3 are in error. The static-pressure and total-pressure contours are also plotted for the cases of $Re = 400$ and 1000 in Figs. 4 and 5. These contour plots are useful, since they are obtained from the solution of the complete Poisson equation so that other approximate solutions could be compared against them.

Two pertinent points are worth observing now: 1) a majority of the finite-difference solutions do not satisfy the no-slip boundary condition to second-order accuracy, and 2) on the other hand, in the velocity-pressure system, it is not the local dilation term, but only the time-rate of change of local dilation, i.e., $\partial D/\partial t$, that is guaranteed to approach zero at convergence.

Finally, it should be pointed out that, in the present work, no attempt has yet been made to analyze the efficiency of the present solutions of (u,v,p) system relative to other available methods; indeed, a study such as that of Atias et al.[7] would be very useful. Nevertheless, it is to be noted that a grid of 29×29 required 1 min of computing time on the IBM 370/168 computer for $Re = 100$ and 4 min for $Re = 1000$, the corresponding time for a 57×57 grid for $Re = 1000$ is 13 min.

In summarizing the work, it can be stated that the numerical solutions obtained are accurate and highly efficient; the efficiency of these solutions is comparable to that of the (ω,ψ) system. The present results for the pressure constitute the first accurate solutions of the Neumann problem using coordinate transformations. The mapping functions used provide a suitable mesh-point distribution and can be used for many internal flow configurations. All results in the present work are obtained using a totally central-difference scheme. Therefore, the solutions do not suffer from the false-diffusion characteristics inherent in the first-order accurate upwind differencing scheme and thus do not misrepresent the associated physical transport processes.

Acknowledgment

This research was performed while the first author was a Visiting Scientist at Air Force Flight Dynamics Laboratory, WPAFB, Ohio, under Technology Inc. and University of Dayton Contracts. The authors are thankful to U. Ghia for her many suggestions and discussions and to R. K. Goyal for

giving his valuable time in generating some of the results and the computer plots for this paper.

References

[1] Roache, P. J., "Recent Developments and Problem Areas in Computational Fluid Dynamics," *Lecture Notes in Mathematics*, Vol. 461, Springer-Verlag, New York, 1975.

[2] Ghia, K. N., Hankey Jr., W. L., and Hodge, J. K., "Study of Incompressible Navier-Stokes Equations in Primitive Variables Using Implicit Numerical Technique," AIAA Paper 77-648, 1977.

[3] Burggraf, O. R., "Analytical and Numerical Studies of the Structure of Steady Separated Flows," *Journal of Fluid Mechanics*, Vol. 24, Pt. 1, Jan. 1966, pp. 113-151.

[4] Bozeman, J. D. and Dalton, C., "Numerical Study of Viscous Flow in a Cavity," *Journal of Computational Physics*, Vol. 12, No. 3, July 1973, pp. 348-363.

[5] Rubin, S. G. and Harris, J. E., "Numerical Studies of Incompressible Viscous Flow in a Driven Cavity," NASA SP-378, 1975.

[6] Kawaguti, M., "Numerical Solution of the Navier-Stokes Equations for the Flow in a Two-Dimensional Cavity," *Journal of the Physical Society of Japan*, Vol. 16, Nov. 1961, pp. 2307-2315.

[7] Atias, M., Wolfshtein, M., and Israeli, M., "A Study of the Efficiency of Various Navier-Stokes Solvers," *AIAA Journal*, Vol. 15, Feb. 1977, pp. 263-266.

[8] DeVahl Davis, G. and Mallison, G. D., "An Evaluation of Upwind and Central Difference Approximations by a Study of Recirculating Flow," *Computers & Fluids*, Vol. 4, 1976, pp. 29-43.

[9] Mills, R. D., "Numerical Solutions of the Viscous Flow Equations in a Class of Closed Flows," *Journal of Royal Aeronautical Society*, Vol. 69, Dec. 1965, pp. 714-718.

[10] Pan, F. and Acrivos, A., "A Steady Flows in Rectangular Cavities," *Journal of Fluid Mechanics*, Vol. 28, Pt. 4, June 1967, pp. 643-655.

[11] Davis, R. T., Ghia, U., and Ghia, K. N., "Laminar Incompressible Flow Past Sharp Wedges," *Computers & Fluids*, Vol. 2, 1974, pp. 225-235.

[12] Ghia, U. and Goyal, R. K., "A Study of Laminar Recirculating Flow in a Driven Cavity of Polar Cross-Sections," *Numerical/Laboratory Computer Methods in Fluid Mechanics*, edited by A. A. Pouring, 1976, pp. 73-91.

Effects of Axial and Radial Air Injection on the Near Wake with and without External Compression

D. H. Neale,* J. E. Hubbartt,† and W. C. Strahle‡
Georgia Institute of Technology, Atlanta, Ga.

Introduction

EXPERIMENTS and analysis show that the base pressure of blunt-based bodies at supersonic speeds can be increased by initiating a zone of combustion adjacent to the base region. Efficient operation has been demonstrated using the concept of "base burning" in which fuel reacts in the near-wake shear flow.[1,2] Experience shows, however, that the maximum base pressure with this mode of operation approximately equals the freestream pressure and that efficiency decreases with increasing base pressure. Base thrust (i.e., base pressure higher than the freestream pressure) is possible using "external burning" in which the fuel combusts in the exterior inviscid flow surrounding the wake.[3,4] The economics of this mode of operation, however, remains uncertain. It is currently thought that a combination of base and external burning offers the greatest promise for achieving base thrust. Although evidence indicates that these modes of burning can be superimposed,[5] efficient performance is yet to be verified.

Results from the second phase of an experimental program to study base pressure enhancement are reported in the present Note. Reference 6 documents the first phase of testing which defines base pressure trends and near-wake structure detail for systematic variations in the freestream flowfield simulating external burning. Freestream manipulation was achieved with a series of axisymmetric and asymmetric test section wall contours translated relative to the model base plane. The contours were designed to focus compression fields on the near wake, representing some reasonable total heat addition in the exterior flow at different rates of release. Further base pressure and near-wake structure measurements are presented here both for radial and base injection of cold air. These tests were conducted to evaluate flow phenomena arising from actual injection of a secondary fluid and are intended to link the first phase simulation tests with the final program segment in which external and base burning of hydrogen fuel will be investigated.

Test Facility

The axisymmetric test facility was designed to simulate the base flow of a projectile at Mach 3 with a fineness ratio of about 6 and a Reynolds number of 3×10^6. The 5.72-cm-diam model is supported in the upstream subsonic flow and extends through the throat into the test section. Bleed air is ducted into the model through the upstream support struts. Radial jet injection was done though six sonic nozzles located about 0.25 base radii upstream of the base plane and equally spaced around the periphery. A porous, sintered-metal base plate was used for axial injection into the near wake. Details of the test facility, other instrumentation, and experimental techniques and accuracies are discussed in Ref. 6.

Results and Discussion

Radial Jet Injection

The effect of radial, cold-air injection on the base pressure is shown in Fig. 1. Results are shown both for no external compression and for axisymmetric external compression with Compression Section II[6] (which produces a net thrust with no cold-air injection). The important observation is that base pressure P_b decreases with injection rate as a result of the competing effects of vortex generation, flow displacement, and degradation in total pressure by the attendant shock system. The decrease is essentially independent of the nozzle diameter and reaches a maximum of over 10% of the freestream pressure P_1. At lower injection rates the loss in base pressure is somewhat reduced by compression.

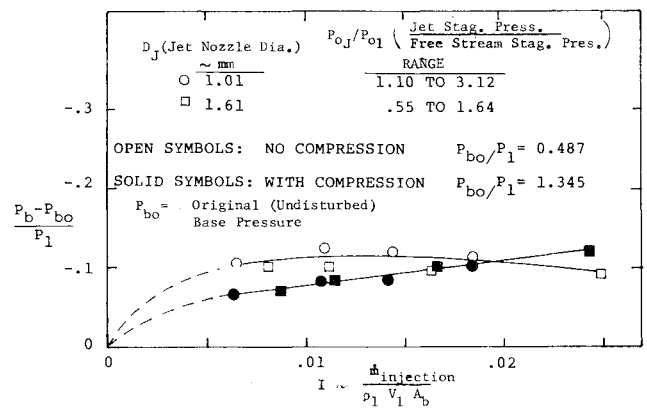

Fig. 1 Effect of radial jet injection on base pressure.

Received June 21, 1978; revision received Oct. 16, 1978.

Index categories: Jets, Wakes, and Viscid-Inviscid Flow Interactions; Airbreathing Propulsion.

*Senior Research Engineer.
†Professor of Aerospace Engineering. Member AIAA.
‡Regents' Professor. Member AIAA.